Key Engineering Materials
ISSN: 1662-9795, Vol. 822, pp 373-380
doi:10.4028/www.scientific.net/KEM.822.373

Submitted: 2019-03-05
Revised: 2019-06-04
Accepted: 2019-06-04
Online: 2019-09-24

Influence of Powder Condition on Surface Properties of Cold-Resistant High-Strength Steel Produced by Direct Laser Deposition Method

Rudolf Korsmik[1,2,a*], Ekaterina Alekseeva[2,b], Alexander Breki[2,c]

[1]Saint-Petersburg State Marine Technical University, St. Petersburg, Russia

[2]Peter the Great St. Petersburg Polytechnic University, St. Petersburg, 195251, Russia

[a]r.korsmik@ltc.ru, [b]alexeeva__ekaterina@mail.ru, [c]albreki@yandex.ru

Keywords: Direct laser deposition, high-strength steel, cold-resistant steel, initial powder condition, corrosion resistance, abrasive-corrosion resistance, wear resistance.

Abstract. Direct laser deposition (DLD) allows creating parts of complex shapes and configurations in a single process step without using of additional equipment. Such technologies are required in the shipbuilding industry, aircrafts, gas turbines, mechanical engineering etc., where it is necessary to manufacture large-sized and complex products that have a long technological cycle for production using classical technologies. DLD makes it possible to produce parts of various alloys with mechanical characteristics at the level of the wrought alloys. The publication is described direct laser deposition of high-strength cold-resistant steels results. Besides mechanical properties of material, the exploitation properties of the structure are also significantly important. Results of corrosion, abrasive-corrosion and tribotechnical tests are shown.

Introduction

Cold-resistant steels are widely used in the Arctic and northern regions for shipbuilding and different marine structures. The main characteristic of using cold-resistant steels is the high resistance to brittle fracture at low temperatures and high corrosion resistance in the seawater. Laser and hybrid laser-arc technologies already have a good results applied for welding of high-strength and cold-resistant steels [1 – 4].

Nowadays, many industries try to introduce the modern technology of part's manufacturing which is based on adding material – additive technologies. The most useful energy source for additive manufacturing is laser irradiation. Additive technologies based on selective laser sintering and selective laser melting (SLS- and SLM technology) [5 - 7] almost ready for practical application. However, SLS and SLM technologies are characterized low productivity and small size of manufacturing parts, which are caused by technological aspects of the process.

The additive technology, which is able to solve these issues, is direct laser deposition (DLD) – the method based on supplying of filler material by compressed gas-powder jet directly into the laser action zone [8]. DLD makes it possible to produce parts of various alloys with mechanical characteristics at the level of the wrought alloys [9 – 16]. High productivity, automation and reduction in total processing time are required in adaptive and flexible manufacturing [17, 18].

DLD process allows creating parts of complex shapes and configurations in a single process step without using of additional equipment. Such technologies are required in the shipbuilding industry, aircrafts, gas turbines, mechanical engineering etc., where it is necessary to manufacture large-sized and complex products that have a long technological cycle for production using classical technologies [8, 19, 20]. The technology has been reducing the consumption of raw materials and the amount of waste. The materials utilization rate for this technology is 70%, there is also the possibility of using secondary and tertiary powder.

Besides mechanical properties of material, the exploitation properties of the structure are also significantly important. This article shows the corrosion, abrasive-corrosion, wear resistance of material manufactured via DLD.

Experimental Procedure

Experimental Equipment. DLD of the high-strength cold-resistant steel was realized on the laser technological machine for cladding and additive manufacturing (Fig. 1).

Laser technological machine based on industrial robot LRM-200iD_7L, Fanuc; laser irradiation source LS 5, IPG Photonics; laser head FLW D30, IPG Photonics with removable cladding nozzle COAX9, Fraunhofer IWS; powder feeder Sulzer Metco Twin 10C with track transection of metering disk of 16×1.2 mm^2.

Figure 1. Laser technological machine for cladding and additive manufacturing.

Using Materials. Steel powder 09CrNi2MoCu fracture of 45-160 μm was used as the feeding material for DLD process. The powder was obtained by gas atomization process. Chemical composition is shown in the Table 1.

Table 1. Chemical compositions (wt%) of the feeding powder 09CrNi2MoCu.

Fe	C	Cr	Ni	Mo	Cu	Si	Mn
Bal.	0.0074	0.64	2.0	0.4	0.6	0.04	0.28
Al	V	N	O	Ca	P	S	-
0.01	0.01	0.008	0.1	0.01	0.02	0.01	-

At the first stage of the study, the technological parameters were determined for as received condition of the powder to ensure the continuity and stability of depositing material. At the second stage, the technological parameters were fixed and condition of the filler powder (as received, 45-160 μm, used, 45-160 μm, mixture of used & unused, 45-160 μm) were varied.

Methods of Inspection. All deposited samples were inspected visually by means of optical and scanning electron microscopy. Corrosion and abrasive corrosion rate were measured by mass loss. The specimens were immersed in a 5% NaCl solution during 240 hours for corrosion testing and in circulating water with the addition of 0.5% silica sand of the 0.4 - 0.8 mm fraction for 1, 3, 5 hours for abrasive corrosion testing. Rectangular slabs triplicate specimens with the size about 55×40×10 mm were tested. Before the measurements, the samples were grinded with 120 grit paper. Then the samples were prepared with the standard method described in ASTM G1-03. The tests were run at ambient temperature.

Corrosion and abrasive-corrosion rate were determined as

$$V=\Delta m \times T/\rho \times S \times t, \quad (1)$$

where Δm is mass loss, T is hours per year, ρ is density, S is the initial area, t is duration of test.

Abrasive corrosion tests were carried using the test vessel equipped with solution supplying system. The speed of flow with solution with sand is 5 meters per second. The direction of flow is perpendicular to a sample.

The tribotechnical test were conducted via spinning friction method using a face friction machine PBD-40 in accordance with the schematic given in figure 2. The rotating counterbody was a cylindrical sample (roller) of ShKh-15 bearing steel with a diameter of 10 mm. During the tests, the rotating counterbody was pressed by its flat side to the plane of the clamped specimen. The clamp, fixed on a bearing knot using a cable and a strain gage within the experiment, was kept from rotation transmitted by the movable roller. In all measurements, the load per friction pair was 85 N, and the rotation frequency of the shaft clamping the steel roller was 200 rpm. Measurements of the trace diameter's changing were carried out with an interval of 1 minute; the total duration of the test for each sample was 5 minutes. Rectangular slabs triplicate specimens with the size about 10×10×10 mm were tested. Before the measurements, the samples were grinded with 120 grit paper.

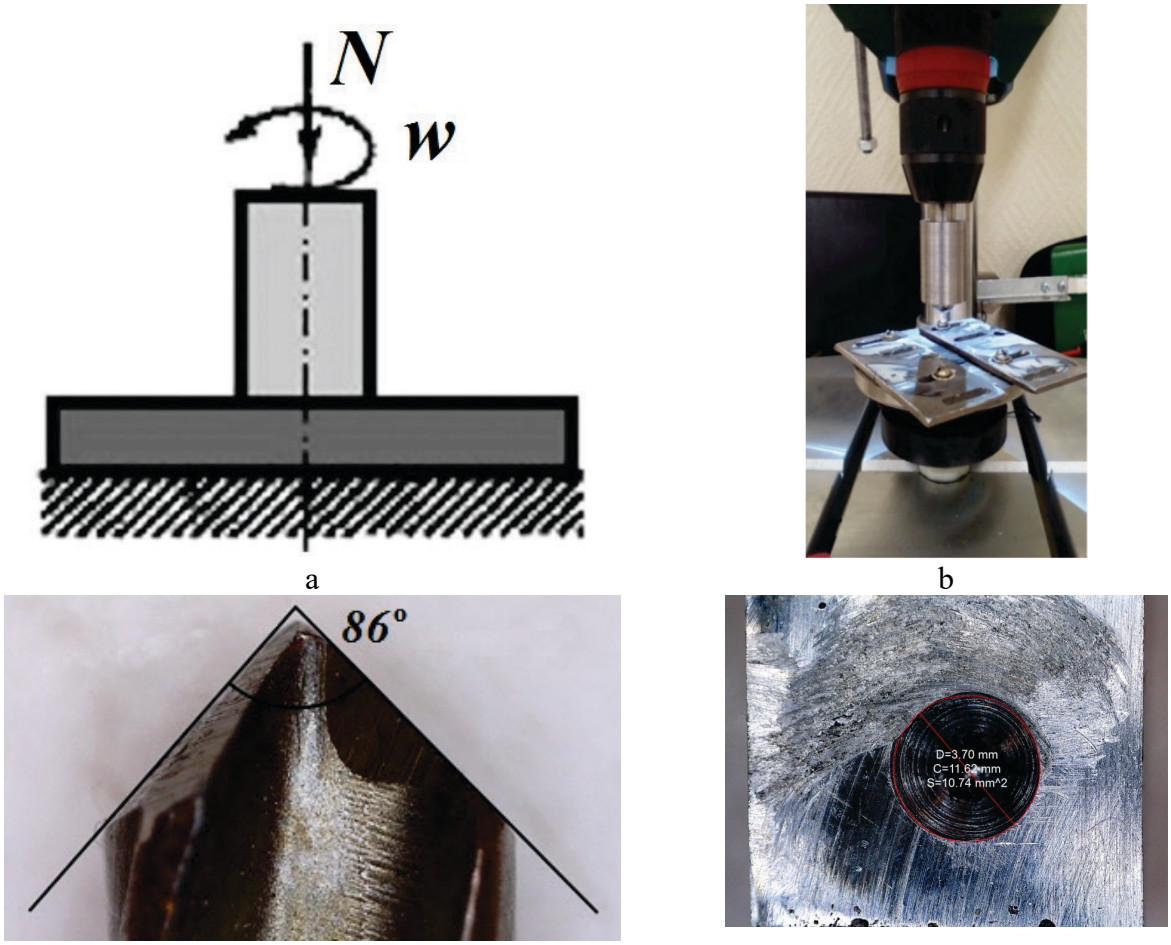

a b c d

Figure 2. Spinning friction method: a) testing scheme, b) testing set up, c) rotating counterbody, d) trace measuring.

Linear wear was calculated as

$$H = (d_n - d_{n-1}) * k_t, \quad (2)$$

where H is linear wear, mm; d_n is actual diameter of trace, mm; d_{n-1} is previous diameter of trace, mm; k_t – transition coefficient from trace diameter to linear wear, which depends on counterbody cone angle α (α=86°, $k_п$= 0,536).

Experimental Results

Corrosion wear. The mass losses of the specimens with different powder condition in 5% NaCl solution and in circulating water with the addition of 0.5% silica sand are reported in Table 2.

Table 2. Test results.

Powder condition	Corrosion test	
	Corrosion rate, mm/year	Average, mm/year
As-received	0.0519	0.0481
	0.0517	
	0.0407	
Used	0.0574	0.0538
	0.0522	
	0.0519	
Mixture of as-received and used	0.0431	0.0431
	0.0414	
	0.0454	

It was found that there is no difference in corrosion rate between the specimens with different types of powder the average corrosion rate for all samples is about 0,04-0,05 mm/year. According to operational documents for the part, which is supposed to be manufactured by the DLD method, the permissible level of corrosive wear for 10 years is 0.6 mm. In the case of our results, corrosive wear for 10 years is 0.43 – 0.54 mm. A clear dependency of the initial powder condition effect on corrosive wear is not found. The surface of samples after testing is shown in figure 3.

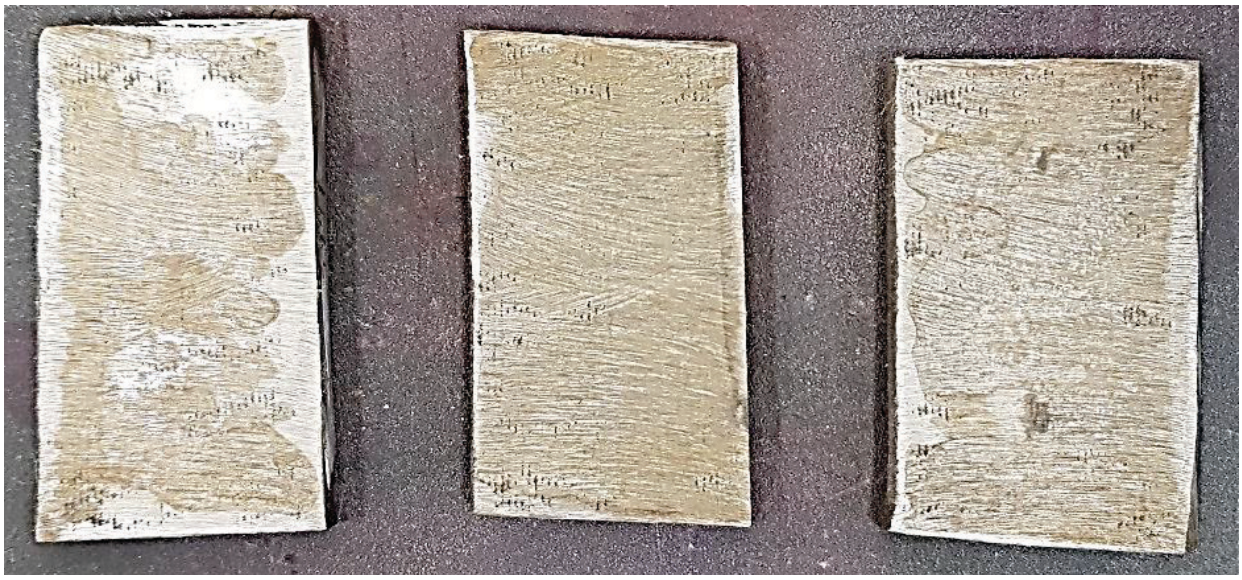

Figure 3. The surface of tested samples.

Abrasive corrosion wear. In result of comparison of the surface of the samples after corrosion-abrasive tests, it can be seen that samples deposited from powders of different initial condition behave in a similar way (figure 4).

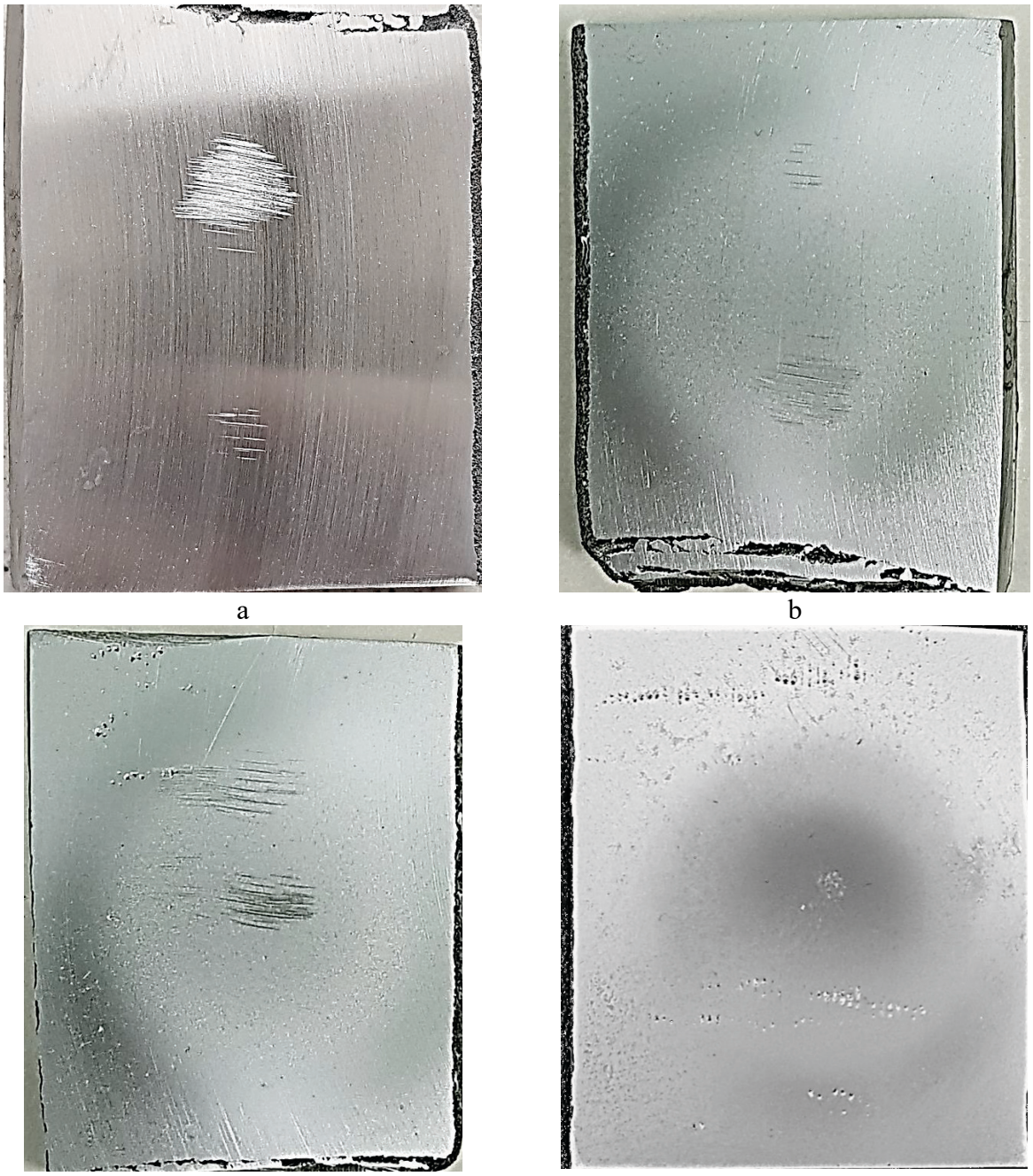

Figure 4. The surface of samples: a) before testing, b) after 1 hour of testing, c) after 3 hours of testing, d) after 5 hours of testing.

After 1 hour of testing, a spot of wear appears on the surface of the samples, corresponding to the diameter of the nozzle (figure 4b). After 3 hours of testing, wear spot becomes more perceptible (figure 4c). Finally, after 5 hours of testing, the wear spot is clearly visible, and metal becomes less shiny, which indicates a significant degree of wear (figure 4d). The results of testing are reported in figure 5.

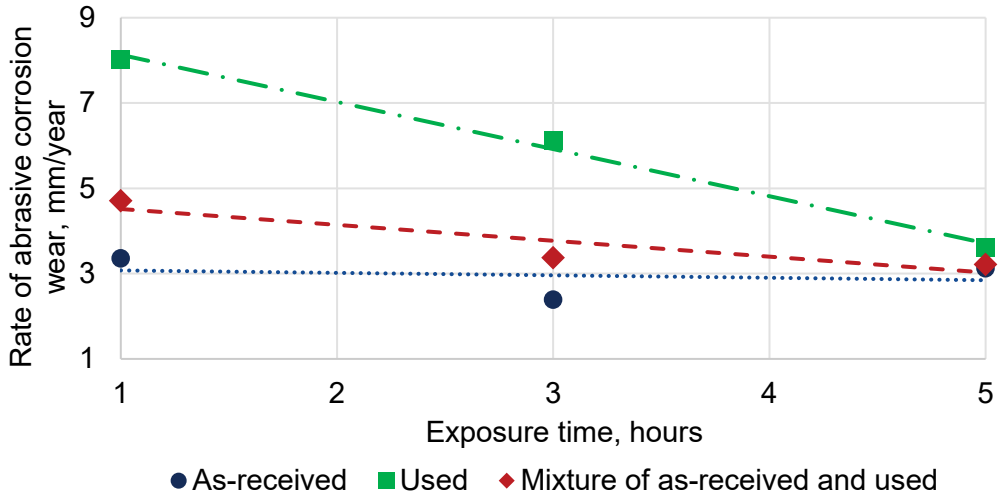

Figure 5. Corrosion-abrasive wear rate during the test.

Abrasive corrosion rate was revealed to be decreasing with the time of exposure (figure 5). Abrasive corrosion rate has the lowest value for the sample made with as received powder. During the increasing of used powder concentration in the filling material, the wear of surface goes higher. Nevertheless, with enlarging test duration up to 5 hours, the results tend to a single value. It can be assumed, that during long-term exploitation of the structure, the influence of the filler powder quality parameters is not significant.

Tribotechnical properties. It was found that there is no difference in spinning friction wear between the specimens with different types of powder. Measured diameters of traces for all samples are in range of $1.8358\sqrt{t} \leq D \leq 1.9675\sqrt{t}$, where D is trace diameter, mm; t is time, min. The changes of trace diameters after friction testing are presented in figure 6. A clear dependency of the initial powder condition effect on spinning friction wear is not found.

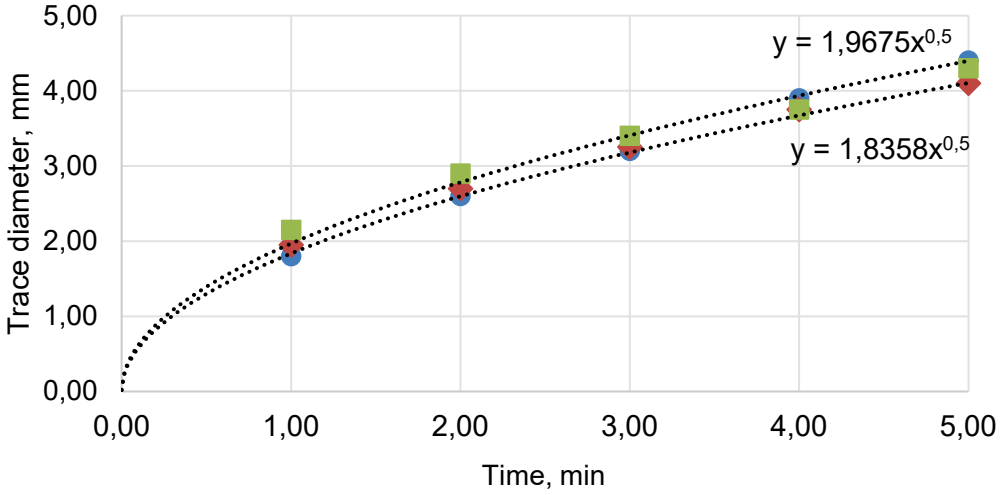

Figure 6. The change of trace diameter during the testing time.

To transfer values of trace diameters to linear wear, the formula (2) was used. The results of calculated linear wear are shown in figure 7. The linear wear is in range of $0.2439t \leq H \leq 0.327t$. These results corresponds with steel materials this type of strength and wear resistance.

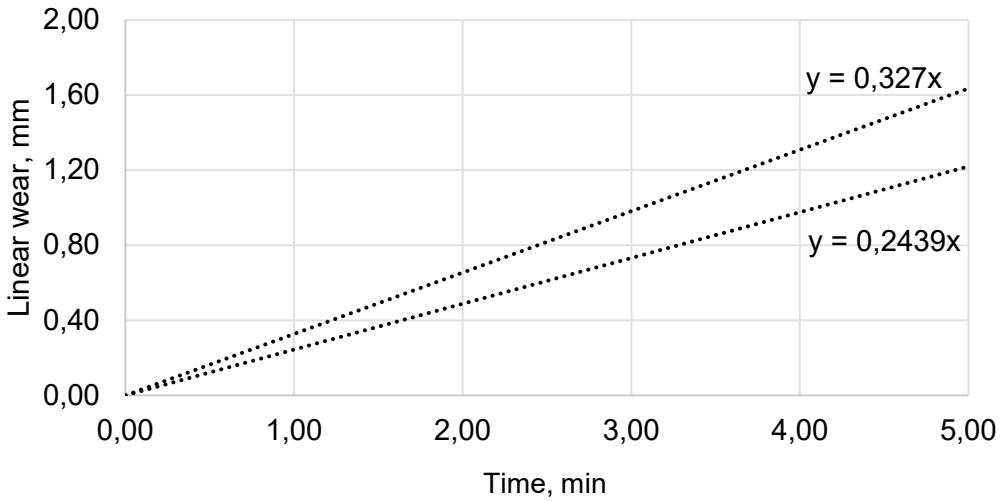

Figure 7. Linear wear of deposited samples.

Conclusions

Increasing of used powder concentration raises the corrosion-abrasive wear of the samples. However, prolongation of exposure time, the abrasive wear for samples deposited from different powder conditions becomes almost the same.

Corrosion and spinning friction wear resistance for all samples deposited from different powder conditions corresponds with the materials obtained by conventional technologies of drowning and casting.

Acknowledgment

The work is carried out with the financial support of the state by the Ministry of education and science of the Russian Federation. Unique project identifier: RFMEFI57417X0175.

References

[1] Turichin G, Kuznetsov M., Klimova-Korsmik O., et al. Laser-Arc hybrid welding perspective ultra-high strength steels: influence of the chemical composition of weld metal on microstructure and mechanical properties // Procedia CIRP. 2018 Jan 1; 74: 752-6.

[2] Sokolov M., Salminen A., Khlusova E.I., et al. Testing of new materials and computer aided optimization of laser beam welding of high-strength steels // Physics Procedia. 2015 Jan 1; 78: 255-64.

[3] Turichin G., Kuznetsov M., Tsibulskiy I., et al. Hybrid Laser-Arc Welding of the High-Strength Shipbuilding Steels: Equipment and Technology // Physics Procedia. 2017 Dec 31; 89: 156-63.

[4] Turichin G., Kuznetsov M., Sokolov M., et al. Hybrid laser arc welding of X80 steel: influence of welding speed and preheating on the microstructure and mechanical properties // Physics Procedia. 2015 Jan 1; 78: 35-44.

[5] Olakanmi, E.O., Cochrane, R.F., Dalgarno, K.W., A review on selective laser sintering/ melting (SLS/SLM) of aluminum alloy powders: Processing, microstructure, and properties//Progress in Materials Science. 2015. vol. 74. pp. 401-477.

[6] Safin, D.Y., Future Engineering of Russia // Sbornik trudov Vseross. Conf. molodich uchenich I specialistov. Moscow, 28 sentyabrya – 01 octyabrya 2011. MGTU im. N.E. Baumana. 2011. 332 p.

[7] SLM Solutions focuses on aviation repair // Metal Powder Report. 2015. vol. 70. iss. 2. 94 p.

[8] Turichin G.A., Klimova O.G., Zemlyakov E.V., et al. Technological Aspects of High Speed Direct Laser Deposition Based on Heterophase Powder Metallurgy // Physics Procedia. 2015. №78. pp. 397-406.
[9] Thompson S.M., Bian L., Shamsaei N., et al. An overview of Direct Laser Deposition for additive manufacturing; Part I: Transport phenomena, modeling and diagnostics // Additive Manufacturing. 2015. №8: 36-62.
[10] Zhang, K., Wang, S.J., Liu, W.J., et al. Characterization of stainless steel parts by Laser Metal Deposition Shaping // Materials and Design. 2014. №55. pp. 104-119.
[11] Gharbi M., Peyre P., Gorny C., et al. Influence of various process conditions on surface finishes induced by the direct metal deposition laser technique on a Ti–6Al–4V alloy // Journal of Material Processing Technology. 2013. №213. pp. 791-800.
[12] Mazumder, J., Song, L.J. Advances in direct metal deposition, in: ASME 2013 International Mechanical Engineering Congress and Exposition, Article number V02AT02A012, 2013.
[13] Gasper A.N.D., Catchpole-Smith, S., Clare, A.T. In-situ synthesis of titanium aluminides by direct metal deposition // Journal of Material Processing Technology. 2017. №239. pp. 230-239.
[14] Shalnova S.A., Klimova-Korsmik O.G., Sklyar M.O. Influence of the Roughness on the Mechanical Properties of Ti-6Al-4V Products Prepared by Direct Laser Deposition Technology // InSolid State Phenomena. 2018. vol. 284. pp. 312-318.
[15] Sklyar M.O., Klimova-Korsmik O.G., Turichin G.A., et al. Influence of Technological Parameters of Direct Laser Deposition Process on the Structure and Properties of Deposited Products from Alloy Ti-6Al-4V // InSolid State Phenomena. 2018. vol. 284. pp. 306-311.
[16] Sklyar M.O., Klimova-Korsmik O.G., Cheverikin V.V. Formation Structure and Properties of Parts from Titanium Alloys Produced by Direct Laser Deposition // Solid State Phenomena. 2017. Mar 1; 265.
[17] Radziwon A., Bilberg A., Bogers M., et al. The smart factory: exploring adaptive and flexible manufacturing solutions // Processing Engineering. 2014. №69. pp. 1184-1190.
[18] Turichin G.A., Zemlyakov E.V., Klimova O.G., et al. Direct laser deposition – perspective additive technology for aircraft engine // Svarka I diagnostika. 2015. №3. pp. 54-57.
[19] Guo, P., Zou, B., Huang, C.Z., et al. Study on microstructure, mechanical properties and machinability of efficiently additive manufactured AISI 316L stainless steel by high-power direct laser deposition // Journal of Material Processing Technology. 2017. №240. pp. 12-22.
[20] Sklyar M.O., Turichin G.A., Klimova O.G., et al. Microstructure of 316L stainless steel components produced by direct laser deposition // Steel, in Translation. 2016. №46. pp. 883-887.
[21] Luzhnov Yu.M., Aleksandrov V.D. Bases of triboengineering: edited by Yu.M. Luzhnov. / Moscow: MADI. 2013. 136 p.

Available online at www.sciencedirect.com

ScienceDirect

Procedia Manufacturing 36 (2019) 249–255

Procedia MANUFACTURING

www.elsevier.com/locate/procedia

17th Nordic Laser Material Processing Conference (NOLAMP17), 27 – 29 August 2019

Microstructure and Mechanical Properties of Laser Metal Deposited Cold-Resistant Steel for Arctic Application

R. Mendagaliyev[a], G.A. Turichin[b], O.G. Klimova-Korsmik[a,b,*], O.G. Zotov[a], A.D. Eremeev[a,b]

[a] *Peter the Great St. Petersburg Polytechnic University, St. Petersburg 195251, Russia*
[b] *Saint Petersburg State Marine Technical University, St. Petersburg 190121, Russia*

Abstract

The article presents the study of the direct laser deposition (DLD) process of cold-resistant steel 09CrNi2MoCu (F620W). As a result, many bainite transformation products are produced. The formation of a bainitic structure in the process of deposition is still little studied; in the process of the growth of the deposited wall, the microstructure undergoes a phase transformation. The work details the equipment for direct laser deposition, describes the main technological parameters of the regime, and studies the surface of the steel powder. Mechanical tests for impact toughness were carried out at a temperature of −40°C, with different laser emission powers. The results are given using the initial powder, as well as used powder with a different mixing ratio, and the results are analyzed. As a result of the study, it was established that the fractional composition of the F620W alloy powder has a significant effect on the mechanical characteristics of samples obtained by direct laser deposition. The effect of recycled powder on the mechanical properties of the samples obtained is given.

Peer-review under responsibility of the scientific committee of the 17th Nordic Laser Material Processing Conference.

Keywords: Direct laser deposition; Direct metal deposition; Cold resistant steel; Arctic; Additive technology; High strength steel; Microstructure; Bainite structures; Toughness.

* Corresponding author. Tel.: +7-952-355-5043; fax: +7812-5529843.
E-mail address: o.klimova@ltc.ru

2351-9789
Peer-review under responsibility of the scientific committee of the 17th Nordic Laser Material Processing Conference.
10.1016/j.promfg.2019.08.032

1. Introduction

Currently, the main task of the development of shipbuilding and engineering is to improve the quality and speed of production of complex parts using additive manufacturing. Direct laser deposition DLD (DMD direct metal deposition analogue) has the ability to produce products with complex shape from various materials [1, 2]. Manufacturing of parts by laser direct deposition (DLD) [3-5] is one of the promising areas of the 21st century, based on the layer-by-layer deposition of metal powder in the zone of laser exposure. Such technology can be applied to materials used in Arctic conditions. The main reason for using cold-resistant steels is the high resistance to brittle fracture at low temperatures [6].

In shipbuilding, cold-resistant steel is using for propeller brackets, stem, and other structures for work on the Arctic shelf. Parts and products can be manufactured in one technological step and are not inferior in quality to parts manufactured by traditional methods [7-11]. Unlike traditional technology, using a DLD, a bainitic microstructure can be achieved. The presence of a bainitic structure should provide higher viscous properties, reduce brittleness, which is very important for cold-resistant steels. At the same time, the DLD technology can allow to regulate the process of formation of bainitic structures and ensure the production of bainite with the required morphology [12–13].

High-strength steel with a bainite structure is one of the most used materials in shipbuilding, since its properties have a good balance of high strength and toughness. According to the literature, there is a huge amount of research devoted to the study of bainite formation, including kinetics, microstructural morphology, crystallography and related mechanical properties [14]. Nevertheless, many theoretical questions about this microstructure are still being discussed, although various types of bainitic steels have been introduced into various industries [15, 16].

The article presents the results of studies of structure formation in steel of bainite class, obtained using the DLD process. The effect of process parameters on the formation of bainite structures was studied. The possibility of using additive methods for manufacturing products with satisfactory mechanical characteristics is demonstrated.

2. Materials and research methodic

The study samples obtained by the DLD method are investigated. The equipment is a robotic complex based on an industrial robot LRM-200iD_7L, Fanuc; laser emission LS-5 IPG Photonics; FLW D30 IPG Photonics laser head with removable surfacing nozzle COAX9 Fraunhofer IWS; powder feeder SulzerMetco Twin 10C.

During the study, the following samples were obtained with variable irradiation power P = 1400 W, 2000 W, 2300 W and constant deposition rate 32 mm/s, which determined by values of traverse speed, powder feeding rate, X increment after each bead and Z increment after each layer.

Samples for metallography and impact toughness were cut from a single slab with the following dimensions: (height = 65 mm; width = 48 mm; thickness = 11.2 mm). Samples for the study of the microstructure were made by cold casting into a conductive resin. To identify the microstructure, chemical etching was used in a 10% alcohol - based H_2NO_3 solution, the etching time was 3–10 seconds (9 ml of alcohol C_2H_5OH + 1 ml HNO_3). The structure was studied using a PhenomProX electron microscope and a LOMO Metam LV-31 optical microscope.

The pendulum impact tester RKP 450 was used to determine the toughness. The size of the pits and oxide inclusions in fractures was measured in Digimizer Image Analysis Software.

The starting material is a powder alloy F620W (09CrNi2MoCu) produced by SphereM (Figure 1) – shipbuilding, high-strength and cold-resistant steel, an economically alloyed. Chemical composition is presented in Table 1.

Table 1. Chemical composition of steel F620W.

Material	C	Si	Mn	Cr	Ni	Mo	S	P	Al	Fe	Cu	Ca
F620W	0,08 - 0,11	0,17 - 0,37	0,30 - 0,60	0,30 - 0,70	1,80 - 2,20	0,35	0,01	0,015	0,01 - 0,05	All the rest	0,40 - 0,70	0,03

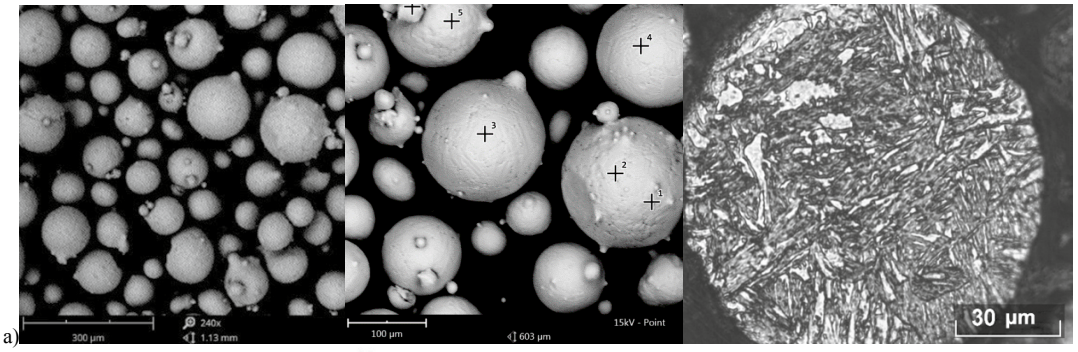

a)

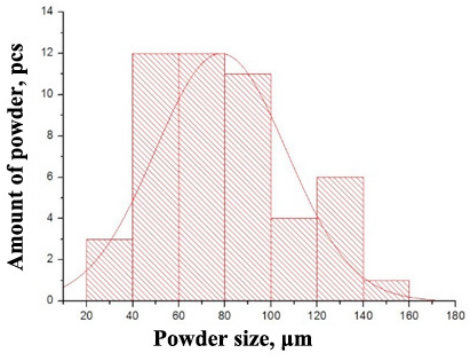

b)

Fig. 1. SphereM powder 45-160 µm, a) surface of powder particles; b) particle distribution histogram.

Table 2 presents the results of the study of the surface of the powder.

Table 2. Powder parameters.

Powder	Average satellite size, (µm)	Sphericity	Number of satellites	Flow rate of powder, (g/s)
		Powder fraction 45-160 µm		
«SphereM»	21,26	0,95	On 5 particles 2 satellite	3,72

3. Sample microstructure

With an increase in power from 1400 W to 2000 W and 2300 W, grain growth is observed, the structure in some areas represents the bainitic ferritic component Figure 2.

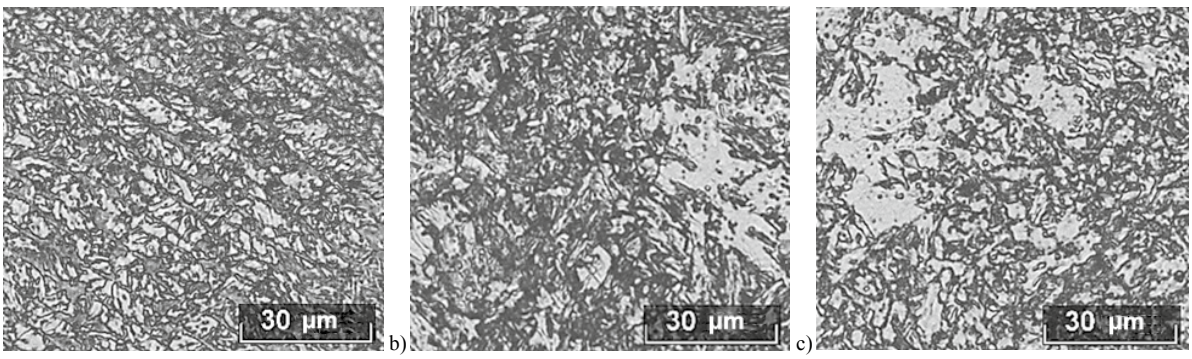

a) b) c)

Fig. 2. Microstructure formation at power, a) P = 1400 W, b) P = 2000 W, c) P = 2300 W.

Figure 3 shows the microstructures obtained with a radiation power of 2000 W, observed in different parts of the

deposition wall. Depending on the cooling rate, the transformed microstructures are complex and may contain upper bainite (UB), granular bainite (GB) with different morphology, and in some cases polygonal ferrite (PF) [16].

Granular bainite (GB) – grains of irregular shape, sometimes plates in which a dislocation structure is observed, packages of parallel plates characteristic of upper bainite are missing. This type of ferrite forms at lower cooling rates than acicular ferrite. Upper bainite (UB) of periodic type with a structure of parallel spaced strips or plates. The second structural component is along the boundaries of the ferritic plates of the M/A-phase (martensitic-austenitic mixture), carbides plates (if M/A is present, it is characterized as degenerate). The formation of a bainitic structure begins with the isolation of embryos of upper bainite along the boundaries of austenitic grains, which are almost completely preserved in the bainitic structure [17-19].

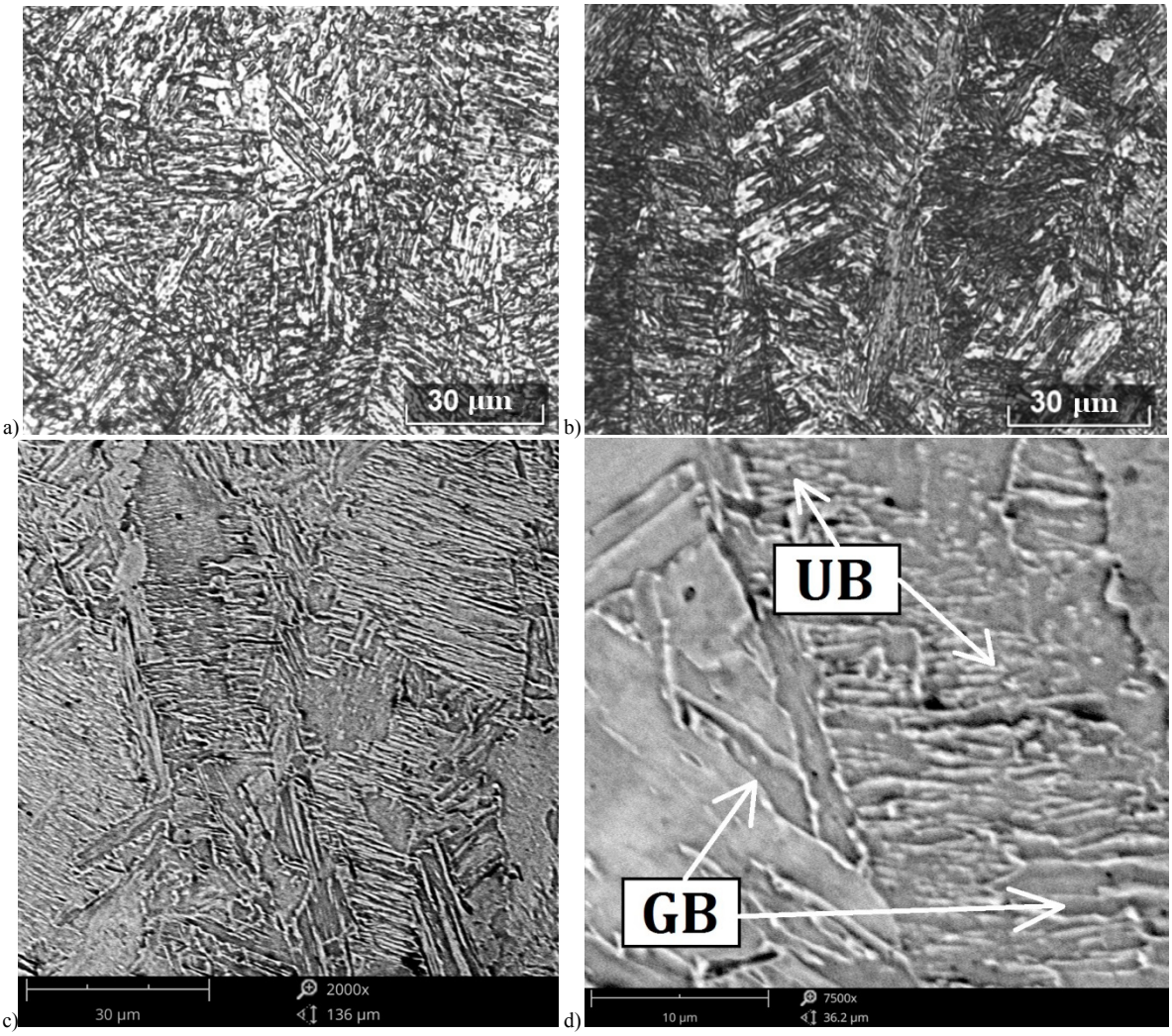

Fig. 3. Microstructure, a, b) optical microscope (bainite); c, d) electron microscope upper bainite (UB), granular bainite (GB).

4. Mechanical tests of the obtained samples

To study the toughness of material produced via DLD process, the specimens were obtained with deposition rate was 32 mm/s and varied laser power from 1400 W to 2300 W from powder with different condition (as-received, used and its mixture), Table 3.

Table 3. Modes DLD.

No.	P, (W)	Powder	T, (^{0}C)	K, (J)	KCV^{-40}, (J/cm^2)
Z/1.1	1400	As-received	-40	60,1	73,3
Z/1.3		Used		24,53	29,6
Z/1.4		As-received + Used (50/50)		28,3	34,3
Z/1.6	2300	As-received		69,6	86,3
Z/1.7		Used		43,36	53,3
Z/1.8				41,63	50,6
Z/1.10	2000	As-received + Used (50/50)		17,56	22
Z/1.12		As-received		67,96	84,66

Figure 4 shows the individual fracture surfaces of specimens obtained by the DLD method after the impact toughness. The presented fractographs of the samples indicate that the fractures are predominantly ductile fracture. With a low laser emission in the process of deposition, a large number of defects in fractures appear in the samples, such as cracks and oxide inclusions.

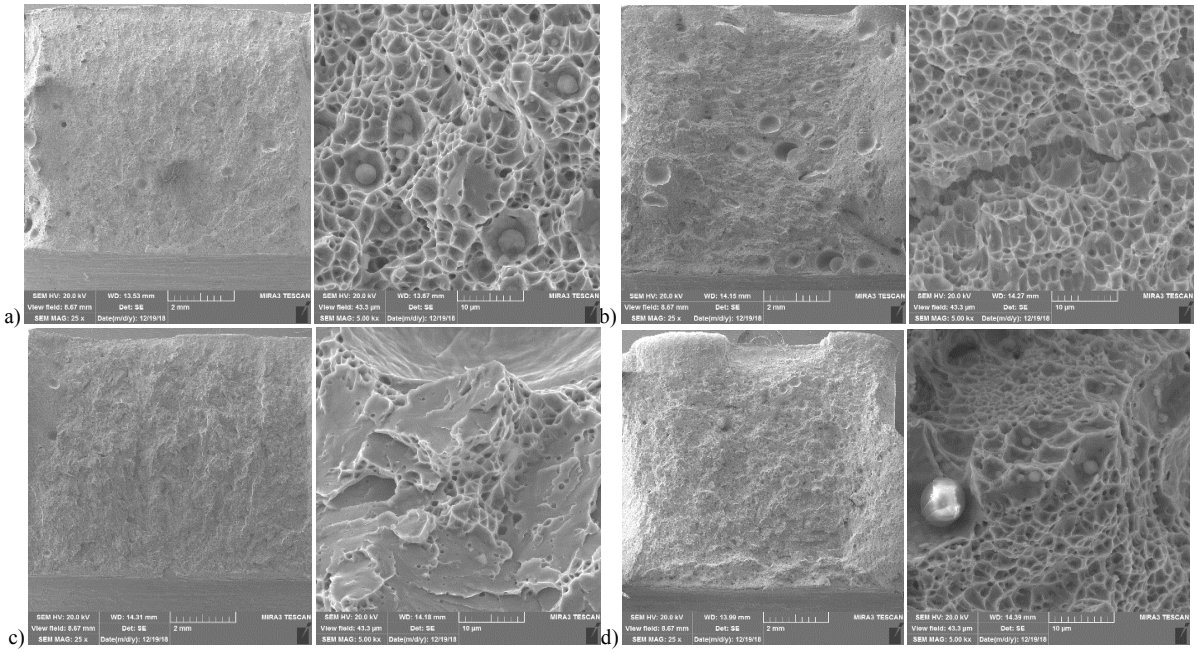

Fig. 4. Fractographs of the obtained samples, a) Z/1.3 b) Z/1.7 c) Z/1.10 d) Z/1.12.

Equaxial pits form in fractures, ductile failure, finely dispersed oxides are present, a larger number and larger size of oxide inclusions are found in Table 4. The pits originated at the interface between the matrix and globular inclusions, which can be particles of sulfides and oxides in rare cases there are nitrides.

Table 4. - Fracture analysis.

No.	Average hole size (μm)	Average oxide size (μm)
Z/1.3	2,49	1,1
Z/1.7	1,85	0,6
Z/1.10	1,43	0,49
Z/1.12	2,02	1,11

Fracture analysis showed in the sample Z/1.3 the average size of the pits is 2.49 μm, the average size of the oxides 1.1 μm; in sample Z/1.7, the average size of the dimples is 1.85 μm, the average oxide size is 0.6 μm; in sample Z/1.10, the average size of the is 1.43 μm, the average oxide size is 0.49 μm; in sample Z/1.12, the average size of the is 2.02 μm, the average size of the oxides is 1.11 μm.

5. Conclusions

The research results demonstrated the possibilities of direct laser deposition production from cold-resistant steels on the example of F620W. The main advantage of the technology is the ability to obtain the necessary structure by regulating the main technological parameters of the process.

The optimal modes of DLD process with high toughness and tensile strength and the microstructure of bainite without martensitic component have been developed. Despite the identified amount of contamination on the surface of the particles of the secondary powder, the mechanical properties of the samples were on a level with samples of the primary powder. This leads to save raw material and, therefore, to reduce the cost of the final product, which is an advantage of the of direct laser deposition process.

With an increase in power from 1400 W to 2000 W and 2300 W, grain growth is observed, the microstructure in some areas is bainitic-ferritic. With a power of 2000 W, the direct laser growth process is optimal and stable, as well as more economical due to the lower laser power; the microstructure is uniform in combination with high mechanical properties.Based on the results of the toughness, several samples with the best values can be noted, exactly: (P = 2300 W) Z/1.6 KCV = 86.3 J/cm^2; (P = 2000 W) Z/1.12 KCV = 84.66 J/cm^2. In this regard, it is advisable to use the mode at power P = 2000 W and deposition rate of 32 mm/s, which is economically justified and affects the final cost of the resulting product**.**

Acknowledgements

The work was carried out with financial support from the Ministry of Education and Science of the Russian Federation within the realization of complex project "Development of direct laser deposition and repair laser cladding technologies of high-strength marine engineering parts operated in the Arctic". Unique identifier of the project RFMEFI57417X0175.

References

[1] J. Mazumder, 1 - Laser-aided direct metal deposition of metals and alloys, Laser Additive Manufacturing, Materials, Design, Technologies, and Applications Woodhead Publishing Series in Electronic and Optical Materials, (2017) 21-53.

[2] Tingting Guan, Suiyuan Chen, Xueting Chen, Jing Liang, Changsheng Liu, Mei Wang, Effect of laser incident energy on microstructures and mechanical properties of 12CrNi2Y alloy steel by direct laser deposition, Journal of Materials Science & Technology, 35 (2019) 395-402.

[3] Grinin O.I, Valdaytseva E.A, Lasota I.T, Pevzner Y, Somonov V.V., Technology of Selective Laser Melting Formation of Heterogeneous Powder Structures, Key Engineering Materials, 736 (2017) 91-94.

[4] G.A. Turichin, O.G. Klimova, E.V. Zemlyakov, K.D. Babkin, D. Yu. Kolodyazhnyy, F.A. Shamray, A.Ya. Travyanov, P.V. Petrovskiy, Technological Aspects of High Speed Direct Laser Deposition Based on Heterophase Powder Metallurgy, Physics Procedia, 78 (2015) 397-406.

[5] G. Turichin, O. Klimova-Korsmik, Theory and Technology of Direct Laser Deposition, Additive Manufacturing of High-

performance Metals and Alloys, (2018) 71-88.
[6] J. Choi, Y. Chang, Characteristics of laser aided direct metal, material deposition process for tool steel, International Journal of Machine Tools and Manufacture, 45 (2005) 597-607.
[7] Klimova-Korsmik O, Turichin G, Zemlyakov E, Babkin K, Petrovsky P, Travyanov A., Technology of High-speed Direct Laser Deposition from Ni-based Super alloys, Physics Procedia, 83 (2016) 716-722.
[8] S. Bhattacharya, G.P. Dinda, A.K. Dasgupta, J. Mazumder, Microstructural evolution of AISI 4340 steel during Direct Metal Deposition process, Materials Science and Engineering: A, 528 (2011) 2309-2318.
[9] T. DebRoy, H.L. Wei, J.S. Zuback, T. Mukherjee, J.W. Elmer, J.O. Milewski, A.M. Beese, A. Wilson-Heid, A. De, W. Zhang, Additive manufacturing of metallic components - Process, structure and properties, Progress in Materials Science, 92 (2017) 112-224.
[10] S.M. Thompson, L Bian, N. Shamsaei, A. Yadollahi, An overview of Direct Laser Deposition for additive manufacturing; Part I: Transport phenomena, modeling and diagnostics, Additive Manufacturing, 8 (2015) 36-62.
[11] Mohammad Ansari, AlirezaMohamadizadeh, Yuze Huang, Vladimir Paserin, EhsanToyserkani, Laser directed energy deposition of water-atomized iron powder: Process optimization and microstructure of single-tracks, Optics & Laser Technology, 112 (2019) 485-493.
[12] G.F. Sun, S. Bhattacharya, G.P. Dinda, A. Dasgupta, J. Mazumder, Influence of processing parameters on lattice parameters in laser deposited tool alloy steel, Materials Science and Engineering: A, 528 (2011) 5141-5145.
[13] Yue Zhou, Suiyuan Chen, Xueting Chen, Tong Cui, Jing Liang, Changsheng Liu, The evolution of bainite and mechanical properties of direct laser deposition 12CrNi2 alloy steel at different laser power, Materials Science and Engineering: A, 742 (2019) 150-161.
[14] B.M.Gurumurthy, Sathya Shankar Sharma, AchuthaKini, Ferrite-Bainite Dual Phase Structure and Mechanical Characterization of AISI 4340 Steel, materialstoday proceedings, 5, (2018) 24907-24914
[15] Chiradeep Ghosh, ClodualdoAranas Jr., John J. Jonas, Dynamic transformation of deformed austenite at temperatures above the Ae3, Progress in Materials Science, 82 (2016) 151-233.
[16] M. Olasolo, P. Uranga, J. M. Rodriguez-Ibabe, B. López, Effect of austenite microstructure and cooling rate on transformation characteristics in a low carbon Nb–V microalloyed steel, Materials Science and Engineering: A, 528 (2011) 2559-2569.
[17] Morteza Toloui, Matthias Militzer, Phase field modeling of the simultaneous formation of bainite and ferrite in TRIP steel, ActaMaterialia, 144 (2018) 786-800.
[18] Yan Chen, Dantian Zhang, Yongchang Liu, Huijun Li, Dakun Xu Effect of dissolution and precipitation of Nb on the formation of acicular ferrite, bainite ferrite in low-carbon HSLA steels, Materials Characterization, 84 (2013) 232-239.
[19] M. Sokolov, A. Salminen, E. I. Khlusova, M. M. Pronin, M. Golubeva, M. Kuznetsov, Testing of New Materials and Computer Aided Optimization of Laser Beam Welding of High-Strength Steels, Physics Procedia, 78 (2015) 255-264.

Key Engineering Materials
ISSN: 1662-9795, Vol. 822, pp 410-417

Submitted: 2019-03-06
Revised: 2019-06-04
Accepted: 2019-06-04
Online: 2019-09-24

Effect of Process Parameters on Microstructure and Mechanical Properties of Direct Laser Deposited Cold-Resistant Steel 09CrNi2MoCu for Arctic Application

Ruslan Mendagaliyev[1,a*], Sergey Yuryevich Ivanov[1,b],
Svetlana Georgievna Petrova[2,c]

[1]Peter the Great St.Petersburg Polytechnic University, St. Petersburg 195251, Russia

[2]Saint Petersburg State Marine Technical University, St. Petersburg 190121, Russia

[a]ruslanm888@mail.ru, [b]ivanov_ftim@mail.ru, [c]psg1@yandex.ru

Keywords: direct laser deposition, Cold resistant steel, Arctic structures, Additive technology, High strength steel, Thermal cycle, Microstructure, Hardness.

Abstract. Effect of process parameters of microstructure formation and mechanical properties of direct laser deposited parts of cold-resistant steel 09CrNi2MoCu is studied. Due to local properties of buildup depends on thermal cycle during fabrication simulation of temperature field was carried out. The following cases were analysed: deposition of the first layer on massive substrate and deposition of a layer on the buildup far from the substrate. It was established that one time high temperature reheating of deposited layer has no effect on hardness while additional reheating up to lower temperature leads to considerable decrease in hardness by 87-100 HV. Far from substrate hardness and microstructure bands of 0.7-0.8 mm thickness have a hardness variation in the range of 250-300 HV. The area close to the substrate has a microstructure of upper bainite with higher hardness due to higher cooling rates during deposition. In the process of deposited, at a higher power, a quick process of heating and cooling occurs, and vice versa, which forms various products of bainite transformation. From the obtained modes were presented the results of tests for impact strength at low temperatures.

Introduction

Steel is widely used in shipbuilding, mechanical engineering, aircraft manufacturing and aerospace industry due to their universal properties. Direct laser deposition (DLD) makes it possible to obtain parts from various alloys with different wall thicknesses, surpassing the physic mechanical properties of parts made by traditional production technologies [1-7]. The fabrication of parts from cold-resistant steel is one of the newest areas of production of the 21st century, which are widely used in the Arctic and northern regions, strategically important areas of production. Details such as pipeline joint assemblies [8, 9], ships and offshore platforms [10], low-temperature high-strength steel materials that can withstand critical loads under extreme conditions [11]. High performance, automation and reduction of total processing time - these functions which are required in adaptive and flexible production environments can be achieved using the DLD method [12-16]. At this moment one of the major problems is to develop optimal process parameters for obtaining parts with high strength and homogeneous microstructure. It should be taking into account that fabricated parts will be used in Arctic conditions. Another problem is to determine relationship between thermal cycles during deposition and microstructure formation.

The aim of the present work is to study effect of process parameters of microstructure formation and mechanical properties of direct laser deposited parts of cold-resistant steel 09CrNi2MoCu.

Experimental Procedure

The samples of steel 09CrNi2MoCu were obtained by DLD. Chemical composition and X-ray analysis of the powder is presented in Table 1. The direct laser deposition system consisted Fanuc robot equipped with a 3 kW fiber laser and coaxial powder nozzle. Process parameters was the

following: beam power 1.4-2.3 kW, forward speed 25 mm s^{-1}, powder flow rate 35.8 g min^{-1}. The average layer height and width resulted to 0.8 mm and 1.6 mm respectively.

Microstructure study was carried out using samples etched in a 9 ml of alcohol C_2H_5OH + 1 ml of HNO_3 solution during 3–10 seconds.

Table 1 Chemical composition of steel 09CrNi2MoCu

Material	C	Si	Mn	Cr	Ni	Mo	S	P	Al	Fe	Cu	Ca
Wrought 09CrNi2MoCu	0.08 - 0.11	0.17-0.37	0.3-0.6	0.3-0.7	1.8-2.2	0.35	0.01	0.015	0.01-0.05	All the rest	0.4-0.7	0.03
Powder (average value)	-	0.55	0.8	0.55	2	-	-	-	-		-	-

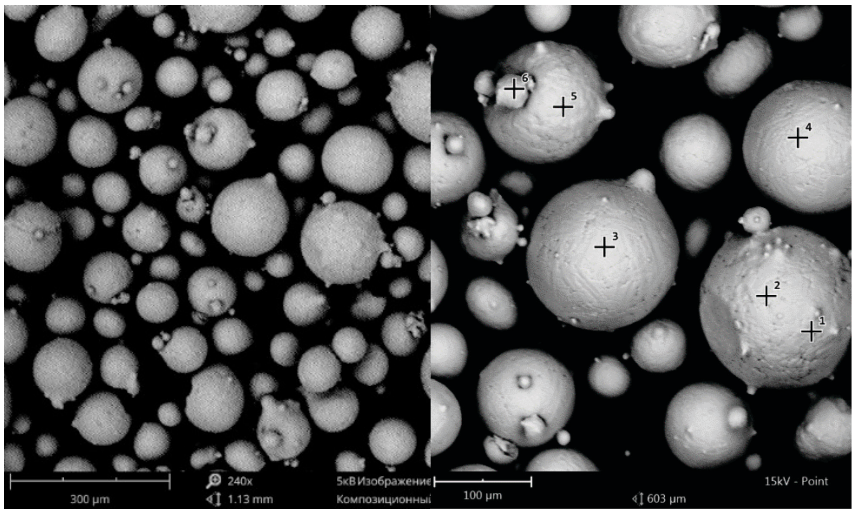

Fig. 1 The surface of the powder particles

Analysis of temperature field during deposition of multilayer wall

In order to determine cooling rates in single pass multilayer wall simulation of temperature field was carried out. The following cases were analysed: deposition of the first layer on massive substrate and deposition of a layer on the buildup far from the substrate. Heat conduction problem was solved by Green's function method. Thermophysical properties were temperature independent. Quasi-stationary solution for moving point heat source in semi-infinite body was used as a fundamental solution. Mirror method was used for obtaining solution for moving point heat source on the edge of the wall. Heat flux of laser beam was described as a normally distributed surface heat source. Calculated cooling curves for different beam power is shown in Fig. 2. It is seen that near substrate deposited layer have a high cooling rates i.e. cooling time in the range 800-500ºC is small. It explained by the intensive heat sink in the massive substrate. It can be assumed that microstructure of buildup near the substrate will have quenched microstructure. Far from the substrate cooling time much longer due to less intensive heat sink. It should lead to formation of more favourable microstructure and properties. It also seen that cooling time may be increased by the increasing the ratio between beam power and deposition speed.

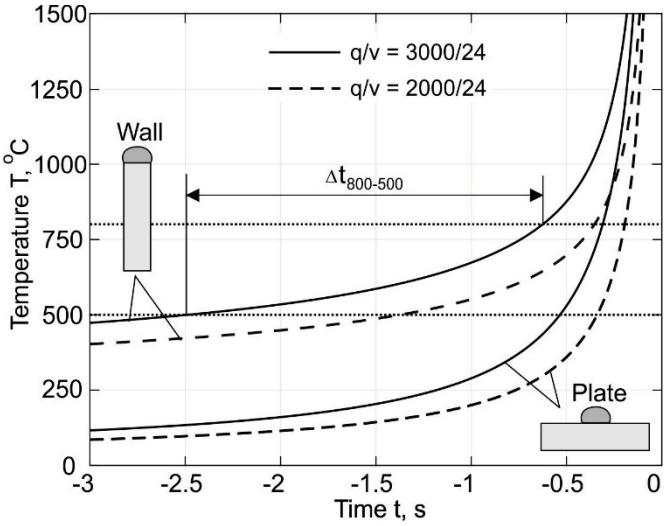

Fig. 2 Cooling curves for a layer deposited on the massive substrate and for a layer deposited on the wall far from substrate

Mechanism of microstructure and properties formation

During of fabrication of large-size parts buildup is considerably cooled down between deposition of layers due to dwell time. Preheating, depending on layer length and process parameters, have considerable effect on cooling rate. How was mentioned above high cooling rates leads to formation of unfavourable microstructure. The following experimental trials were carried out in order to simulate fabrication of large-size part: deposition of single pass wall with cooling buildup down to 50-60°C after each layer. Hardness distribution along the buildup after deposition of six and eight layer is shown in Fig. 3. Microstructure banding is clearly visible on etched macrosamples. The irregular hardness distribution confirms nonuniform behavior of diffusion and microstructural changes. Mechanism of local properties formation can be revealed by the analysis of hardness evolution in points P0-P3, having practically equal distance between each other. Hardness of newly deposited metal in point P0 after deposition of six layers equal to 363 HV. After remelting of this area by the seventh layer, and reheating higher than 1000°C by eight layer hardness remains practically the same. Point P1 in contrast to P0 additionally reheated up to lower temperature by the eight layer. It leads to considerable decrease in hardness by 87 HV to 263 HV. Thermal cycle in point P2 is similar to P1 except additional low temperature reheating that has no effect on hardness. It is also proven by hardness at point P3. It can be concluded that local microhardness depends on thermal cycle during fabrication. One time high temperature reheating of deposited layer has no effect on hardness while additional reheating up to lower temperature leads to considerable decrease in hardness by 87-100 HV. Hardness bands of 0.7-0.8 mm thickness have a hardness variation in the range of 250-300 HV. The area close to the substrate has a higher hardness due ti higher cooling rates during deposition.

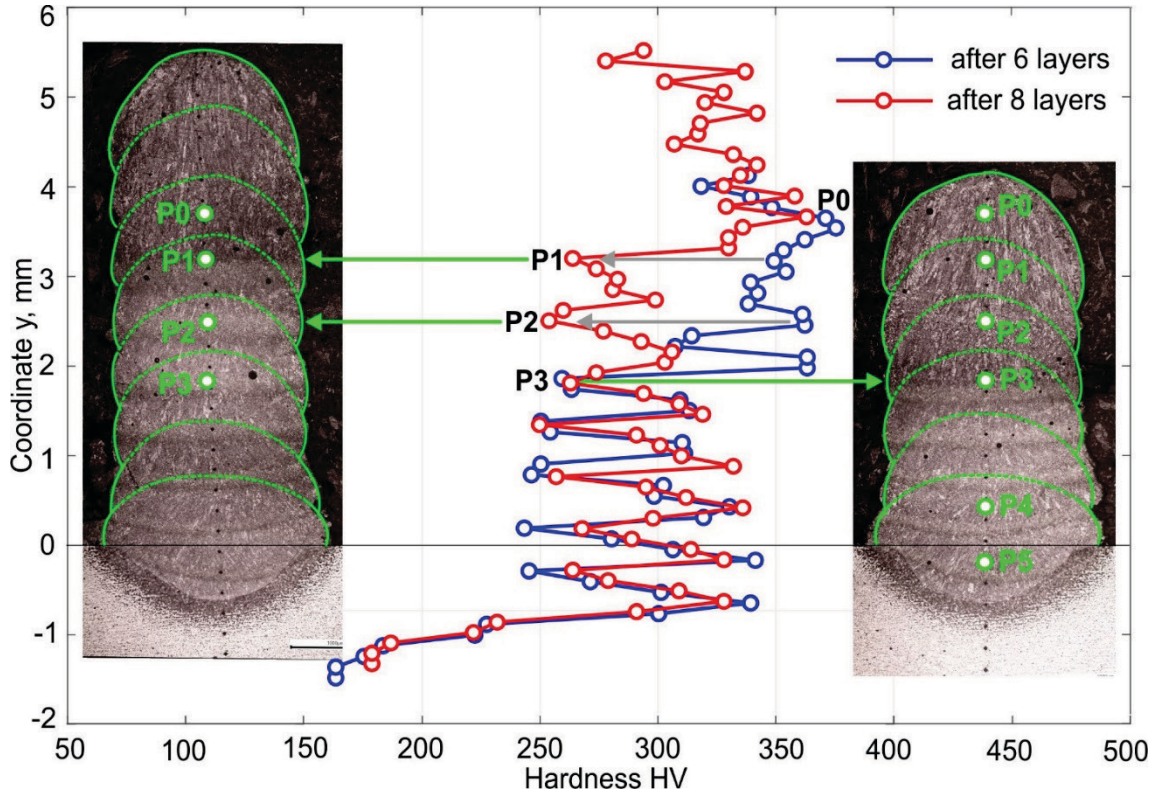

Fig. 3 Hardness distribution along the axis buildup after deposition of six and eight layers respectively

Figure 4 shows several micrographs of the microstructure observed in different parts of the deposited wall (Fig. 3), which corresponds to different cooling rates. Depending on the cooling rate, the transformed microstructures are complex and may contain martensite (M), bainite (B) with different morphology, and in some cases polygonal ferrite (PF). [17, 18].

In the uppers layers of the deposited wall, upper bainite is formed, usually formed in the temperature range from 500-350°C. Particles of carbides are allocated in the form of a batch type with the structure of parallel spaced lathes or plates; the second structural component - along the boundaries of the ferrite plates of the martensite and residual austenite; rod-like carbides nucleation occurs at the boundaries of austenite grains; the boundaries of the former austenitic grains remain.

In the lower part there is a microstructure of lower bainite that forms at lower temperature than upper bainite. Lath morphology; excretion of cementite inside bainitic lathes; the boundaries of the former austenitic grains remain. The lower bainite is usually formed at temperatures of 350 – 200°C and has a needle-like (lamellar) structure. Carbide particles in the lower bainite are located in the α-phase plates.

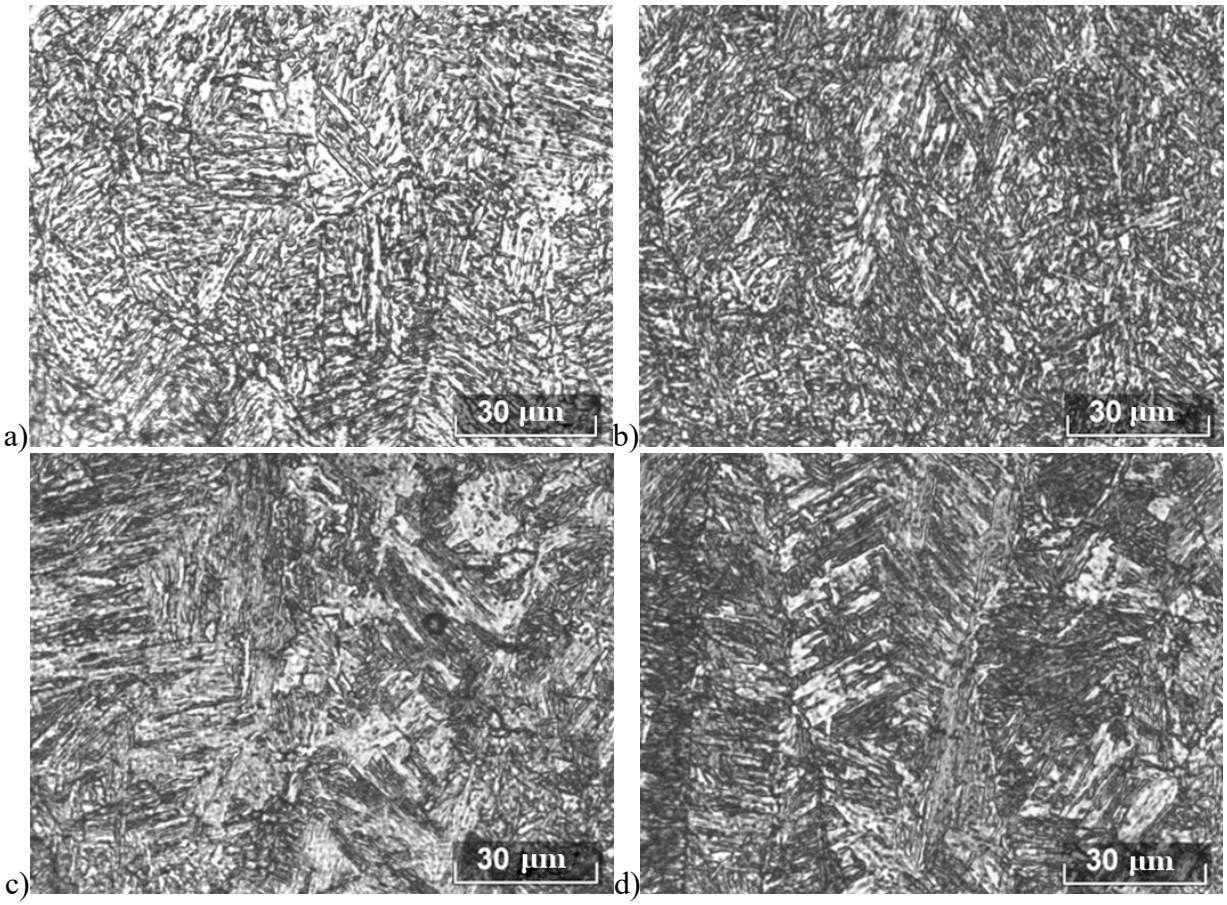

Fig. 4 Microstructure a) zone P5; b) zone P4; c) zone P1; d) zone P0

Table 2 presents results of impact bending test for samples obtained using different laser beam power. Figure 5 shows fractograms of samples after impact bending tests. The fracture (Fig.5a) has a natural ductile fracture and is about 95%, 5% brittle. Equiaxial pits are formed in the fracture. Unmelted particles are also presented. In the fracture (Fig.5b), identical pits are formed, collapsing viscous, finely dispersed oxides are presented, (Fig.5c) a larger amount and a larger size of oxide inclusions are found, compared with the other modes.

Table 2 Fracture toughness

No. mode	P, (W)	Powder sphericity	Fluidity of powder ($g\ s^{-1}$)	K, (J)	KC, ($J\ cm^{-2}$)
1 (a)	1400	0.9528	3,726	50.76	61.6
2 (b)	2000			67.96	84.66
3 (c)	2300			56.3	68

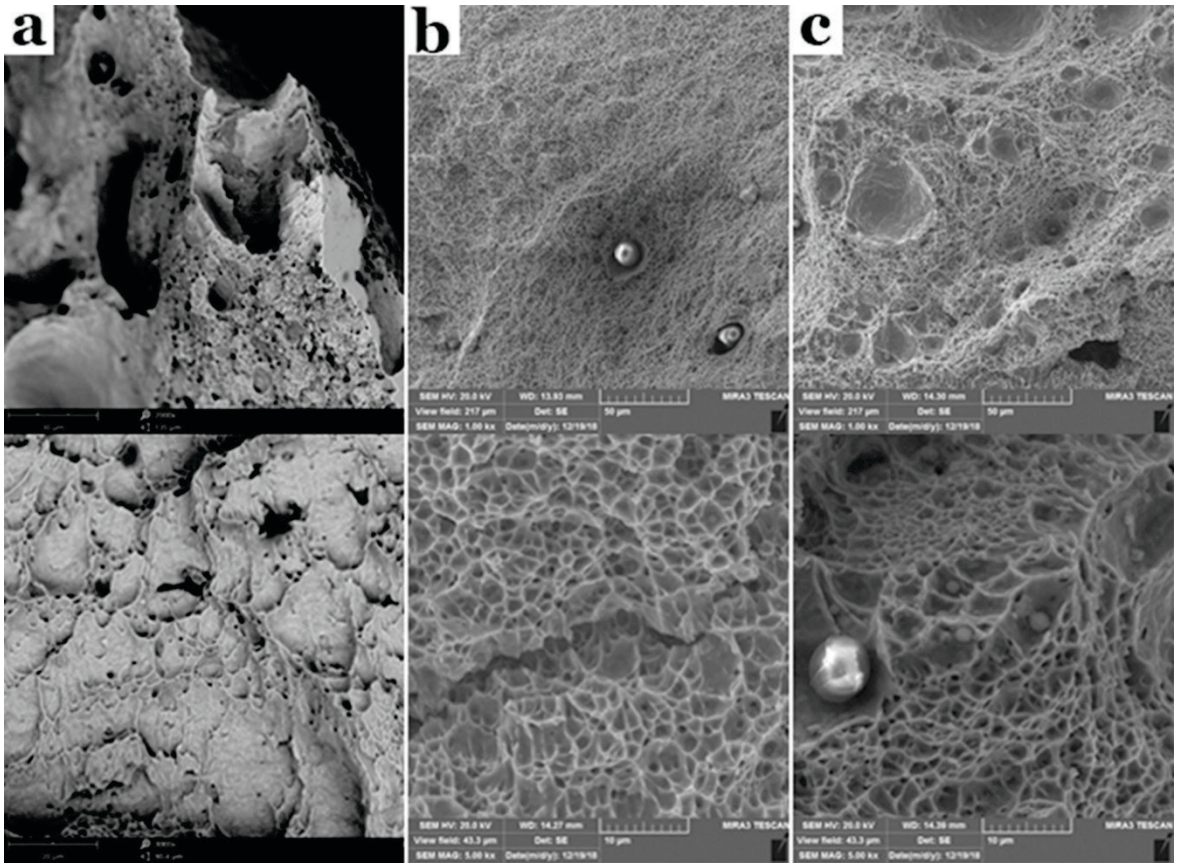

Fig. 5 Fractograms a) P=1400W; b) P=2000W; c) P=2300W

The macrostructure of samples with impact toughness is shown in Figure 6. In sample (a) there are pores with a size of 130-230 μm, non-fusion of 160 μm, in (b) a pore size of up to 160 μm, in (c) a pore size of up to 666 μm.

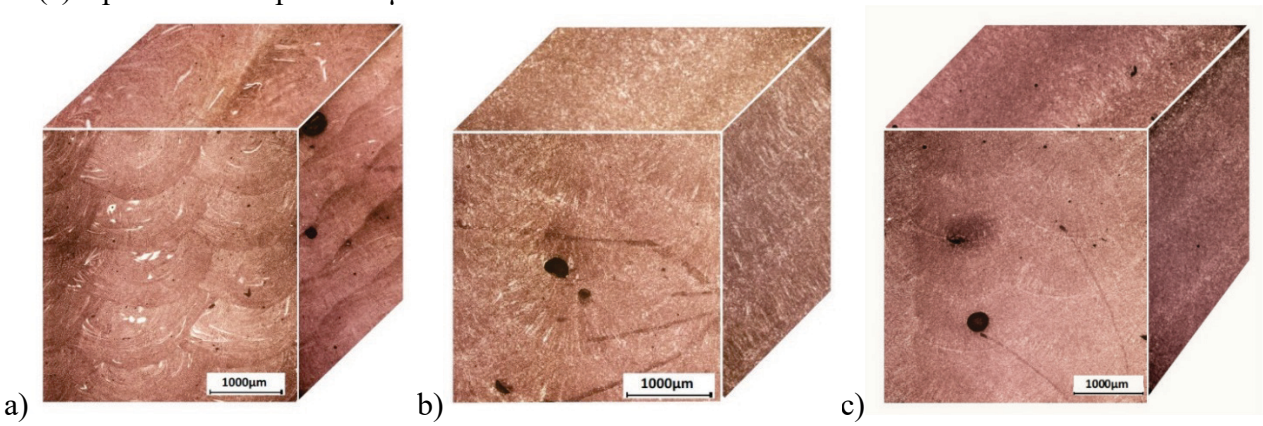

a) b) c)

Fig. 6 3D macrostructure of buildup obtained using beam power 1.4 kW (a), 2.0 kW (b), 2.3 kW (c)

Summary

Local microhardness of buildup depends on thermal cycle during fabrication. One time high temperature reheating of deposited layer has no effect on hardness while additional reheating up to lower temperature leads to considerable decrease in hardness by 87-100 HV. Far from substrate hardness and microstructure bands of 0.7-0.8 mm thickness have a hardness variation in the range of 250-300 HV. The area close to the substrate has a microstructure of lower bainite with a lower hardness due to heat input from the upper layers and lower cooling rates during deposition.

Impact toughness has the best performance when the radiant power is P = 2000W for the given parameters of the deposited process. The impact hardness is predominantly viscous with a small fraction of brittle fracture.

Acknowledgements

The work was carried out with the financial support of the state in the person of the Ministry of Education and Science of Russia - the unique identifier of the work (project) RFMEFI57417X0175.

References

[1] Grinin O.I, Valdaytseva E.A, Lasota I.T, Pevzner Y, Somonov V.V., Technology of Selective Laser Melting Formation of Heterogeneous Powder Structures, Key Engineering Materials. 736 (2017) 91-94.

[2] G.A. Turichin, O.G. Klimova, E.V. Zemlyakov, K.D. Babkin, D. Yu. Kolodyazhnyy, F.A. Shamray, A.Ya. Travyanov, P.V. Petrovskiy, Technological Aspects of High Speed Direct Laser Deposition Based on Heterophase Powder Metallurgy, Physics Procedia. 78 (2015) 397-406.

[3] G. Turichin, O. Klimova-Korsmik, Theory and Technology of Direct Laser Deposition, Additive Manufacturing of High-performance Metals and Alloys. (2018) 71-88.

[4] Klimova-Korsmik O, Turichin G, Zemlyakov E, Babkin K, Petrovsky P, Travyanov A., Technology of High-speed Direct Laser Deposition from Ni-based Super alloys, Physics Procedia. 83 (2016) 716-722.

[5] S. Bhattacharya, G.P. Dinda, A.K. Dasgupta, J. Mazumder, Microstructural evolution of AISI 4340 steel during Direct Metal Deposition process, Materials Science and Engineering: A. 528 (2011) 2309-2318.

[6] T. DebRoy, H.L. Wei, J.S. Zuback, T. Mukherjee, J.W. Elmer, J.O. Milewski, A.M. Beese, A. Wilson-Heid, A. De, W. Zhang, Additive manufacturing of metallic components - Process, structure and properties, Progress in Materials Science. 92 (2017) 112-224.

[7] S.M. Thompson, L Bian, N. Shamsaei, A. Yadollahi, An overview of Direct Laser Deposition for additive manufacturing; Part I: Transport phenomena, modeling and diagnostics, Additive Manufacturing. 8 (2015) 36-62.

[8] Qiang Bai, Yong Bai, 20 - Arctic Pipelines, Subsea Pipeline Design, Analysis, and Installation. (2014) 465-485.

[9] S.V. Panin, P.O. Maruschak, I.V. Vlasov, A.S. Syromyatnikova, A.M.Bolshakov, F. Berto, O. Prentkovskis, B.B. Ovechkin, Effect of Operating Degradation in Arctic Conditions on Physical and Mechanical Properties of 09Mn2Si Pipeline Steel, Procedia Engineering. 178 (2017) 597-603.

[10] Ki Jong Kim, Jong Hwan Lee, Dae Kyeom Park, Bo Gyeong Jung, Xu Han, Jeom Kee Paik, An experimental and numerical study on nonlinear impact responses of steel-plated structures in an Arctic environment, International Journal of Impact Engineering. 93 (2016) 99-115.

[11] Jia-BaoYan, J.Y. Richard Liew, Min-Hong Zhang, Jun-Yan Wang, Mechanical properties of normal strength mild steel and high strength steel S690 in low temperature relevant to Arctic environment, Materials & Design. 61 (2014) 150-159.

[12] A. Radziwon, A. Bilberg, M. Bogers, E. Madsen, The smart factory: exploring adaptive and flexible manufacturing solutions, Procedia Engineering. 69 (2014) 1184-1190.

[13] Sklyar M.O., Turichin G.A., Klimova O.G., Zotov O.G., Topalov I.K., Microstructure of 316L stainless steel components produced by direct laser deposition, Steel in Translation. 46 (2016) 883-887.

[14] Vildanov A.M, Babkin K.D, Zemlyakov E.V, Gushchina M.O., The effects of beam oscillation on the quality of laser deposited metal parts, In Journal of Physics: Conference Series. 1109 (2018) 012059.

[15] Turichin G.A, Somonov V.V, Babkin K.D, Zemlyakov E.V, Klimova O.G., High-Speed Direct Laser Deposition: Technology, Equipment and Materials. 125 (2016) 012009.

[16] Turichin G.A, Klimova O.G, Zemlyakov E.V, Babkin K.D, Kolodyazhnyy D.Y, Shamray F.A, Travyanov A.Y, Petrovskiy P.V., Technological aspects of high speed direct laser deposition based on heterophase powder metallurgy, Physics Procedia. 78 (2015) 397-406.

[17] Chiradeep Ghosh, Clodualdo Aranas Jr., John J. Jonas, Dynamic transformation of deformed austenite at temperatures above the Ae3, Progress in Materials Science. 82 (2016) 151-233.

[18] M. Olasolo, P. Uranga, J. M. Rodriguez-Ibabe, B. López, Effect of austenite microstructure and cooling rate on transformation characteristics in a low carbon Nb–V microalloyed steel, Materials Science and Engineering: A. 528 (2011) 2559-2569.

[19] A.K. Nath, S. Sarkar, Chapter 11-Laser Transformation Hardening of Steel, Advances in Laser Materials Processing (Second Edition). (2018) 257-298.

[20] J.J.S. Dilip, G.D. Janaki Ram, Thomas L. Starr, Brent Stucker, Selective laser melting of HY100 steel: Process parameters, microstructure and mechanical properties, Additive Manufacturing. 13 (2017) 49-60.

[21] Haitham El Kadiri, Liang Wang, Mark F. Horstemeyer, Reza S. Yassar, John T. Berry, Sergio Felicelli, Paul T. Wang, Phase transformations in low-alloy steel laser deposits, Materials Science and Engineering: A. 494 (2008) 10-20.

[22] G. Telasang, J. Dutta Majumdar, G. Padmanabham, M. Tak, I. Manna, Effect of laser parameters on microstructure and hardness of laser clad and tempered AISI H13 tool steel, Surface and Coatings Technology. 258 (2014) 1108-1118.

[23] A.E. Isakov, V.A. Matveeva, M.A. Chukaeva, Development of Chemosorbent Based on Metallic Waste for Cleaning Mine Water From Molybdenum, Journal of Ecological Engeneering. 19 (2018) 42-47.